[4] a) V. A. Ershov, I. Y. Postovskii, *Khim. Geterosikl. Soedin.* **1971**, 571; *Chem. Heterocycl. Compd. (Engl. Transl.)* **1971**, 537; b) E. G. Kovalev, V. A. Anufriev, G. L. Rusinov, *Khim. Geterosikl. Soedin.* **1990**, 1691; *Chem. Heterocycl. Compd. (Engl. Transl.)* **1990**, 1408.

[5] a) M. D. Coburn, G. A. Buntain, B. W. Harris, M. A. Hiskey, K.-Y. Lee, D. G. Ott, *J. Heterocycl. Chem.* **1991**, *28*, 2049; b) C. Glidewell, P. Lightfoot, B. J. L. Royles, D. M. Smith, *J. Chem. Soc. Perkin Trans. 2* **1997**, 1167.

[6] Crystal data for **4** ($C_8H_{16}N_{12}O_2S_2$): $M_r = 376.45$, triclinic, space group $P\bar{1}$; $a = 5.3757(4)$, $b = 9.197(1)$, $c = 9.3683(8)$ Å, $\alpha = 67.564(7)$, $\beta = 75.634(7)$, $\gamma = 76.442(7)^\circ$, $V = 409.65(6)$ Å^3, $Z = 1$, $\rho_{calcd} = 1.526$ mg mm^{-3}; 1392 data measured to $2\theta_{max} = 115^\circ$; $R = 0.0279$, $wR2 = 0.0745$ for all 1106 unique reflections. X-ray intensity data were measured on a Bruker diffractometer with $Cu_{K\alpha}$ radiation ($\lambda = 1.54178$ Å) at $T = 294$ K. The structure were solved with the aid of program XS, and refined with full-matrix least-squares program XL, from SHELXTL software (SHELXTL96 G. M. Sheldrick, *Acta Crystallogr. Sect. A* **1990**, *46*, 467). The XL program minimizes F^2 differences, and uses all data; that is, weak data are not considered "unobserved", and are included in the *R* factors reported. Crystallographic data (excluding structure factors) for the structure reported in this paper have been deposited with the Cambridge Crystallographic Data Centre as supplementary publication no. CCDC-138299. Copies of the data can be obtained free of charge on application to CCDC, 12 Union Road, Cambridge CB2 1EZ, UK (fax: (+44) 1223-336-033; e-mail: deposit@ccdc.cam.ac.uk).

[7] The highest density C,H,N compound reported in the Cambridge Crystallographic Data Centre data base is 5,5′-bi-1*H*-tetrazole (density 1.738 g cm^{-3}): P. J. Steel, *J. Chem. Crystallogr.* **1996**, *26*, 399.

[8] For an explanation of methods for characterizing explosive sensitivity, see R. T. Paine, W. Koestle, T. T. Borek, G. L. Wood, E. A. Pruss, E. N. Duesler, M. A. Hiskey, *Inorg. Chem.* **1999**, *38*, 3738.

[9] S. Rozen, S. Dayan, *Angew. Chem.* **1999**, *111*, 3680–3682; *Angew. Chem. Int. Ed.* **1999**, *38*, 3471–3473.

Synthesis of Prussian Blue Nanoparticles and Nanocrystal Superlattices in Reverse Microemulsions**

Sébastien Vaucher, Mei Li, and Stephen Mann*

Among known molecular magnets, Prussian blue (*catena*-[$MFe^{III}\{Fe^{II}(CN)_6\}$] (M = Li, Na, K, NH_4)) and related cyanometallate-based coordination polymers offer a range of compounds with unique versatility. The variety of structures and magnetic properties of this family of compounds has been extensively investigated,[1] and recently reviewed.[2] Although much work has focused on the relationship between the unit-cell structure and magnetic properties, relatively few attempts have been made towards understanding and controlling the growth mechanism of these magnetic coordination polymers. This is an important aspect in the study of molecular magnets because compounds with appropriate magnetic properties require further fabrication and processing if functional devices and materials are to be produced.

Recently, organic supramolecular templates and organized reaction media have been used for the construction of higher-order assembly of traditional inorganic solids, such as silica,[3] calcium carbonate,[4] and iron oxides.[5] These processes allow the control of properties such as particle size, particle shape, surface texture, and organization to be integrated directly into the synthesis method. It seems feasible that similar strategies could also be developed for the coupled synthesis and construction of both molecular materials and coordination polymers to produce complex functional materials that are organized beyond the length scale of the unit cell. As a first step towards this objective, we address the possibility of coupling the synthesis of Prussian blue crystals with its emergent properties such as size, shape, and higher-order assembly.

Periodically banded arrangements (Liesgang bands) have been produced previously for the precipitation of Prussian blue on perfluorinated membranes.[6] Similarly, a dissipative structure has been briefly reported.[7] More recently, the growth of Prussian blue under Langmuir monolayers[8] and in the interlayer spaces of lamellar vesicles has been described.[9] These studies have focused on the spatial confinement of Prussian blue rather than the colloidal and mesoscale properties of the constituent crystals. Herein, we show that by confining the synthesis to nanoscale water droplets formed in reverse microemulsions prepared from the anionic surfactant sodium bis(2-ethylhexyl)sulfosuccinate (AOT), hydrophobic Prussian blue nanoparticles with a uniform shape and size can be routinely prepared. A related material, $[Cu_2\{Fe(CN)_6\}]$, has been recently synthesized in microemulsion media, although the resulting nanoparticles were highly disorganized.[10] In our experiments, the growth of the nanoparticles within the restricted reaction field is controlled by a multistep process involving the slow photoreduction of $[Fe(C_2O_4)_3]^{3-}$ to produce Fe^{II} ions that subsequently react with $[Fe(CN)_6]^{3-}$ ions to generate nuclei and clusters of Prussian blue encapsulated within the water droplets. Growth of the molecular magnet occurs by further exchange and fusion between microemulsion droplets to produce nanoparticles encapsulated in a shell of surfactant molecules. Moreover, the highly hydrophobic surface properties of the Prussian blue nanoparticles enable the facile preparation of self assembled nanoparticle arrays with 2-D and 3-D superlattice ordering.

AOT reverse microemulsions containing 0.3 M ammonium iron(III) oxalate and 0.3 M ammonium ferricyanide aqueous nanodroplets at $w = 5-20$ ($w = [H_2O]/[AOT]$) were transparent yellow fluids that were stable in the dark at room temperature. Exposure of the microemulsions to daylight transformed them to a transparent blue solution in two days and no precipitate was observed for two weeks. UV/Vis absorption spectra showed a broad band at 680 nm consistent with the Prussian blue $\{Fe^{III}[(t_{2g})^3(e_g)^2]Fe^{II}[(t_{2g})^6]\} \rightarrow \{Fe^{II}[(t_{2g})^4(e_g)^2]Fe^{III}[(t_{2g})^5]\}^*$ electronic transition.[11] FT-IR spectra contained a major band at 2069 cm^{-1} that corresponds to the Fe–CN stretching mode in the cyanometallate lattice.

[*] Prof. S. Mann, Dr. S. Vaucher, M. Li
School of Chemistry
University of Bristol
Bristol BS8 1TS (UK)
Fax: (+44) 117-929-0509
E-mail: s.mann@bris.ac.uk

[**] We thank the Swiss National Science Foundation for a postdoctoral fellowship to S.V. and the University of Bristol for a postgraduate studentship to M.L.

  0570-0833/00/3910-1793 $ 17.50+.50/0

Transmission electron microscopy (TEM) images of samples taken from the blue microemulsions ($w = 15$) after four days showed the presence of cubic Prussian blue nanoparticles with a uniform shape and size that self assembled into 2-D (or 3-D) highly ordered square (cubic) superlattices (Figure 1a). The crystals have a characteristic length of 16 nm on average,

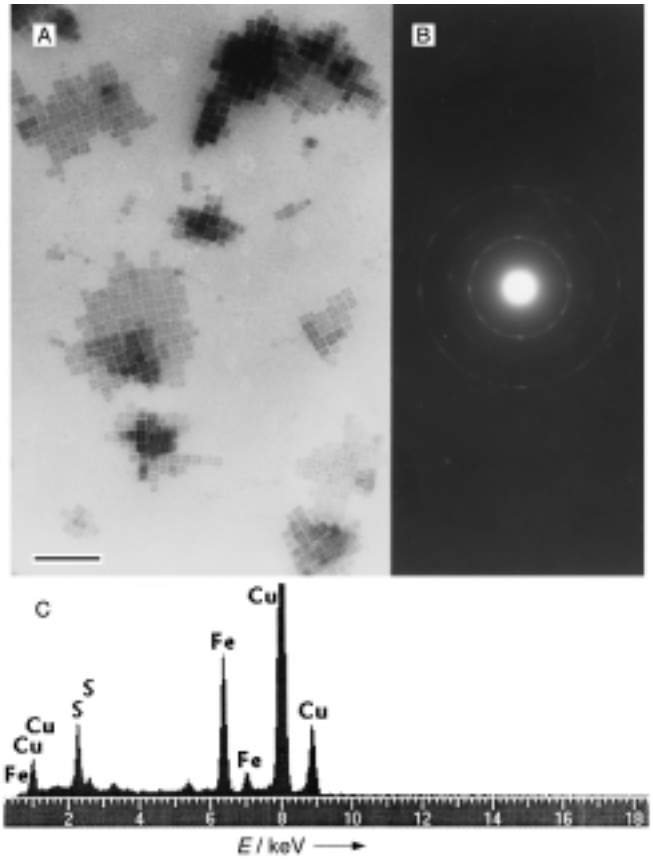

Figure 1. A) TEM image of cubic Prussian blue nanoparticles formed in AOT microemulsions at $w = 15$ showing self assembled 2-D and 3-D superlattices (scale bar 100 nm). B) Electron-diffraction pattern from the superlattice structures showing rings corresponding to the Prussian blue cubic structure; unit cell parameters $a = 1.013$ nm. C) EDXA spectrum of the superlattice structure showing the presence of iron and sulfur, corresponding to Prussian blue crystals and AOT surfactant, respectively. Copper peaks are due to the sample grid.

a narrow particle size distribution σ of 2.7 nm (Figure 2a), and a regular cubic morphology consisting of smooth, well defined faces. Although the nanoparticles were, to some extent, sensitive to the electron beam, electron-diffraction patterns showed d spacings of 2.3, 2.5, 3.6, and 5.1 Å (Figure 1b), which is consistent with a well ordered Prussian blue crystal structure.[12]

Typically, the superlattices were organized in domains up to 200 nm in length (60–100 nanoparticles) while the individual nanoparticles were separated by a regular 2 to 3 nm spacing, which is consistent with an interdigitated bilayer of AOT molecules.[13] The energy-dispersive X-ray microanalysis (EDXA) results show the presence of iron and sulfur (6.4 and 2.3 keV, respectively; Figure 1c), to confirm the presence

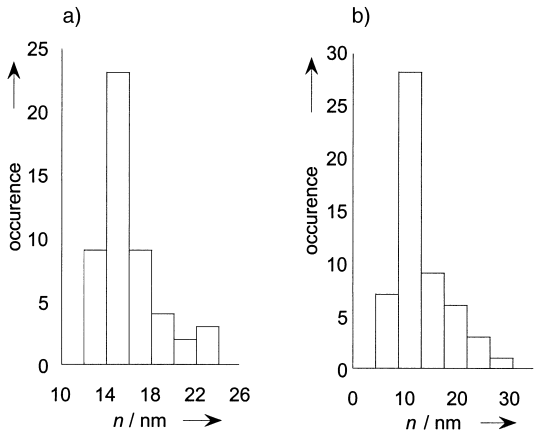

Figure 2. Particle size distributions for Prussian blue nanoparticles formed in AOT microemulsions ($w = 15$, 0.3 M reactants). a) After four days; b) after two days.

of AOT in the Prussian blue nanoparticle array. The self-assembly of the superlattice is therefore a facile process in which the hydrophobic interactions between the surface-adsorbed AOT molecules dominate the interparticle forces during solvent evaporation from the TEM grid. Moreover, the large degree of order in the superlattice domain is a direct consequence of the high concentration of regularly shaped, narrowly distributed Prussian blue nanoparticles produced by undertaking the reaction in organized media. Indeed, the regular cubic morphology indicates minimal interaction between the crystal surfaces and negatively charged AOT headgroups during crystal growth.

These results were in marked contrast to the control experiments. Synthesis in water alone gave a turbid green solution and a blue bulk precipitate that consisted of of large (100–250 nm) discrete cubic particles with a broad size distribution. Reactions in isooctane without AOT produced a phase-separated aqueous blue phase containing crystals similar to those formed in pure water. No product was associated with the isooctane phase.

Formation of the 2-D square superlattice structure from the microemulsion reaction media was time dependent. For example, at $w = 15$ and from 0.3 M reaction solution, samples taken for TEM analysis after two days showed discrete cubic nanoparticles but no long-range ordering (Figure 3a). These particles were smaller and more heterogeneous in size distribution (mean 14 nm, $\sigma = 4.9$ nm) than those collected after four days (Figure 2b) which showed well ordered superlattice structures (Figure 3b). Prussian blue nanoparticles collected from the same microemulsion after two weeks were slightly larger (mean 18 nm, $\sigma = 2.1$) but the domain length of the superlattices was reduced due to the increased number of nanoparticles in the solution (Figure 3c).

The size of the individual nanoparticles was dependent on the concentrations of both the ammonium iron(III) oxalate and ammonium ferricyanide solutions. No significant changes in size (mean 16 nm) were observed at $w = 15$ between concentration values of 0.1–0.3 M. However, at lower concentrations (0.05 M), pale blue, transparent microemulsions were observed after two days in daylight, which transformed

  0570-0833/00/3910-1794 $ 17.50+.50/0

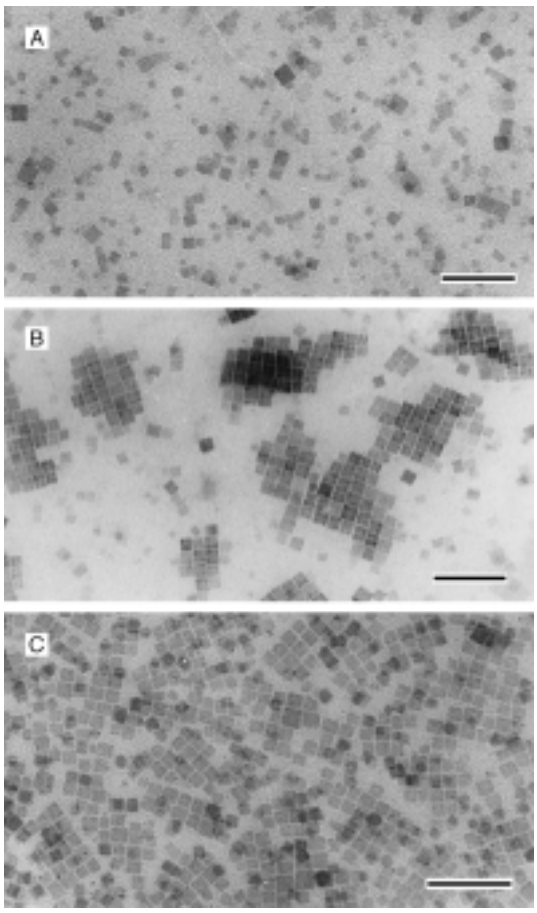

Figure 3. TEM images of discrete Prussian blue nanocrystals formed A) after two days from AOT microemulsions at $w = 15$; B) after four days showing superlattice structures; C) after two weeks, showing well defined crystals but a smaller superlattice domain sizes. Scale bars 100 nm.

into a transparent yellow solution and blue precipitate after three days. The TEM images showed the presence of regular, cubic Prussian blue nanoparticles in the precipitate. The particles had a mean size of 39 nm ($\sigma = 6.1$ nm) and self assembled into superlattice domains (Figure 4a). No blue color developed in the microemulsions at reactant concentrations of 0.01M, although a small yield of superlattice structures, consisting of cubic particles with an average size of 54 nm ($\sigma = 4.2$ nm), were observed (Figure 4b). These observations indicate that below a threshold value of 0.1M, lower reactant concentrations result in fewer crystals of significantly larger dimensions. This is consistent with a nucleation-controlled process of Prussian blue deposition in the microemulsion droplets.

The size of the nanoparticles was reduced when the water content (equivalently, droplet size) of the microemulsions was decreased. For example, discrete cubic particles were synthesized at $w = 10$. These nanoparticles were homogeneous in size (mean 12 nm, $\sigma = 1.4$ nm) and self assembled into small superlattice domains, often consisting of only four to twenty nanoparticles. No nanoparticles were obtained at $w = 5$, most probably because there is only a sufficient amount of water for headgroup hydration (reverse micelles) under these conditions.

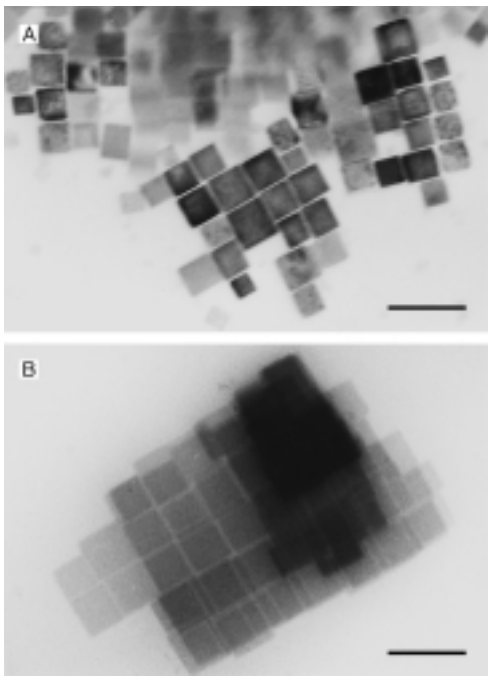

Figure 4. TEM images of Prussian blue nanoparticles and superlattices at $w = 15$ and reactant concentrations of A) 0.05M and B) 0.01M. Scale bars 100 nm.

Control over the size of the Prussian blue crystals clearly depends on various factors such as the rate of nucleation (photoreduction rates and ionic concentrations) and the number of ions of individual water droplets (w values and concentrations). However, at $w > 5$, the nanocrystals are much larger than would be predicted on considering the statistical distribution of reactants among the nanometer-size water droplets. For example, at 0.3M and $w = 15$, we estimate from the known diameter (5.4 nm) of NaAOT microemulsion droplets that there are approximately 15 ions in each water-filled cage.[13] A 16 nm nanoparticle contains approximately 4000 unit cells, that is 16000 $[Fe(CN)_6]^{4-}$ and 16000 Fe^{III} ions. This means that at least 1000 complete transfers would have to take place to produce crystals of the size observed. It remains unclear why the particle size is so uniform. One possibility is that in a given concentration range, the nanoparticle growth is self-limiting. This limitation is imposed by thermodynamic constraints arising from the droplet membrane curvature due to the limited number of water molecules that can be distributed around the crystal surfaces.

The use of in situ photoreduction to prepare nanoparticles and superlattices of molecular magnets from microemulsion fluids could have general applications in photo-patterning processes. For example, photo-formation of Prussian blue has been investigated as an alternative photographic-printing method,[11] and is particularly important when localized reactions and homogenous seeding are required. Studies of photo-patterning of microemulsion thin films is the subject of further investigations.

Experimental Section

Prussian blue was prepared as the mixed valence ammonium cyanometallate $[(NH_4)_xFe_y\{Fe(CN)_6\}]$; $x + 3y = 4$ according to a reported method.[14]

  0570-0833/00/3910-1795 $ 17.50+.50/0

Ammonium iron(III) oxalate ($(NH_4)_3[Fe(C_2O_4)_3]\cdot 3H_2O$, $M_W = 428$; 2.568 g, 6 mmol) was dissolved in hot distilled water (3 mL, 50 °C) contained in a foil-covered flask. Finely powdered potassium ferricyanide ($K_3[Fe(CN)_6]$, $M_W = 329$; 0.987 g, 3 mmol) was added to the hot solution with vigorous stirring for 20 min and then sonicated for 2 min. The solution was left to cool in the dark for several hours. Green crystals of $K_3[Fe(C_2O_4)_3]$ were removed by filtration in the dark from the mixture of $(NH_4)_3[Fe(C_2O_4)_3]$ and $(NH_4)_3[Fe(CN)_6]$ solutions. We used this procedure specifically to remove potassium ions from the reaction mixture as ammonium cyanometallate is significantly more stable than the potassium salt of Prussian blue. The solution was then diluted to 10 mL with distilled water to give an equimolar mixture of $(NH_4)_3[Fe(C_2O_4)_3]$ and $(NH_4)_3[Fe(CN)_6]$ at a concentration of 0.3 M.

A small amount (0.09 – 0.36 mL) of the $(NH_4)_3[Fe(C_2O_4)_3]$ and $(NH_4)_3[Fe(CN)_6]$ mixture (0.01 – 0.3 M in water) was added to an isooctane solution of NaAOT (10 mL, 0.1 M in isooctane) at room temperature in the dark to produce an AOT water-in-oil microemulsions at $w = 5 - 20$. Higher water levels ($w = 15 - 20$) resulted in a slight phase separation of the water in the microemulsion due to the high ionic strength of the reaction solution. This separation could be prevented by using lower concentrations of the reactants. The microemulsions were exposed to daylight for various periods to slowly photoreduce the $[Fe(C_2O_4)_3]^{3-}$ ions to $[Fe(C_2O_4)_3]^{4-}$, which serve as a source of Fe^{II} ions for treatment with aqueous $[Fe(CN)_6]^{3-}$. This latter process is analogous to the Turnbull method for producing Prussian blue.

Samples for analytical TEM and UV/Vis spectroscopy were taken over two weeks. For TEM, droplets of the microemulsion were air-dried onto Formvar-coated, carbon-reinforced, 3 mm diameter, copper electron microscope grids.

Control experiments used equivalent amounts of the $(NH_4)_3[Fe(C_2O_4)_3]$ and $(NH_4)_3[Fe(CN)_6]$ aqueous mixture (0.3 M) added to 10 mL of isooctane or water in the absence of NaAOT.

Received: January 31, 2000 [Z14622]

[1] a) S. Ferlay, T. Mallah, R. Ouahès, P. Veillet, M. Verdaguer, *Nature* **1995**, *378*, 701; b) S. Ohkoshi, Y. Abe, A. Fujishima, K. Hashimoto, *Phys. Rev. Lett.* **1999**, *82*, 1285.

[2] M. Verdaguer, A. Bleutzen, V. Marvaud, J. Vaissermann, M. Seuleiman, C. Desplanches, A. Scullier, C. Train, R. Garde, G. Gelly, C. Lomenech, I. Rosenman, P. Veillet, C. Cartier, F. Villain, *Coord. Chem. Rev.* **1999**, *190 – 192*, 1023.

[3] a) C. T. Kresge, M. E. Leonowicz, W. E. Roth, J. C. Vartuli, J. S. Beck, *Nature* **1992**, *359*, 710; b) S. Mann, S. L. Burkett, S. A. Davis, C. E. Fowler, N. H. Mendelson, S. D. Sims, D. Walsh, N. T. Whilton, *Chem. Mater.* **1998**, *9*, 2300; c) C. G. Göltner, S. Henke, M. C. Weisenberger, M. Antonietti, *Angew. Chem.* **1998**, *110*, 633; *Angew. Chem. Int. Ed.* **1998**, *37*, 613.

[4] a) A. L. Litvin, S. Valiyaveettil, J. Tingle, D. L. Kaplan, S. Mann, *Adv. Mater.* **1997**, *9*, 124; b) D. Walsh , B. Lebeau, S. Mann, *Adv. Mater.* **1999**, *11*, 324.

[5] a) D. D. Archibald, S. Mann, *Nature* **1993**, *364*, 430; b) D. Walsh, S. Mann, *Adv. Mater.* **1997**, *9*, 658.

[6] K. Honda, H. Hayashi, K. Chiba, *Chem. Lett.* **1988**, 191.

[7] D. Avnir, M. L. Kagan, W. Ross, *Chem. Phys. Lett.* **1987**, *135*, 177.

[8] a) S. Ravaine, C. Lafuente, C. Mingotaud, *Langmuir* **1998**, *14*, 6347; b) R. Saliba, B. Agricole, C. Mingotaud, S. Ravaine, *J. Chem. Phys. B* **1999**, *103*, 9712.

[9] Y. Einagam, O. Sato, A. Fujishima, K. Hashimoto, *J. Am. Chem. Soc.* **1999**, *121*, 3745.

[10] S. P. Moulik, G. C. De, A. K. Panda, B. B. Bhowmik A. R. Das, *Langmuir* **1999**, *15*, 8361.

[11] M. Ware, *Cyanotype: The History, Science and Art of Photographic Printing in Prussian Blue*, The Science Museum and the National Museum of Photography, Film and Television, London, **1999**, p. 142, and references therein.

[12] F. Herren, P. Fischer, A. Ludi, W. Haelg, *Inorg. Chem.* **1980**, *19*, 956.

[13] M. Li, H. Schnablegger, S. Mann, *Nature* **1999**, *402*, 393.

[14] M. Ware, *Ag⁺ Photogr.* **1995**, *7*, 74.

Synthesis and Characterization of $Ph_4Te_4I_4$, Containing a Te_4 Square, and $Ph_3PTe(Ph)I$

Philip D. Boyle, Wendy I. Cross, Stephen M. Godfrey,* Charles A. McAuliffe, Robin G. Pritchard, Shamsa Sarwar, and Joanne M. Sheffield

The interaction of organoelement compounds of Group 16 with dihalogens is a subject of considerable current interest. For example, the dihalogen adducts of organoselenium compounds[1, 2] and selenoamides[3–5] have all been intensively studied by a variety of research groups in the last few years. In addition, we have recently reported the structure of $Ph_3PSe(Ph)I$, formed from the reaction of Ph_3P with $Ph_2Se_2I_2$.[6] Many of the dihalogen compounds formed lie close to the ionic/covalent borderline, and several structural types have been identified which are dependent on the substituents R, the donor atom, the identity of the halogen, and, in some cases, the dielectric constant of the solvent in which such compounds are prepared. For example, dimethylselenide diiodine adopts a three-coordinate charge-transfer (CT) structure, $Me_2SeI{-}I$,[1] whereas the corresponding dibromide adopts a disphenoidal "see-saw" structure, Me_2SeBr_2. On the other hand, Me_2SBr_2 is a CT complex, $Me_2SBr{-}Br$, thus illustrating the importance of the donor atom on the nature of the dihalogen adduct produced.[7] Also of relevance to the present study is the isolation of the first stable alkanetellurenyl pseudohalides by Fimml and Sladky, who reported on compounds of formula $(Me_3Si)_3CTeX$ (X = CN, SCN, SeCN, NCO, N_3).[8]

The interaction of Ph_2Se_2 with diiodine has been described by du Mont and co-workers, and a very interesting CT complex was observed in the solid state.[9] The X-ray crystal structure of this molecule revealed a dimeric centrosymmetric moiety containing short and long iodine – iodine distances (2.775(1) and 3.588(1) Å, Figure 1). In view of this interesting (and unexpected) structure, we were interested in synthesizing the analogous tellurium compound from the stoichiometric reaction of Ph_2Te_2 and molecular iodine in diethyl ether in order to determine if the compound produced is isomorphous with $Ph_2Se_2I_2$ or whether a new structural motif would be revealed.

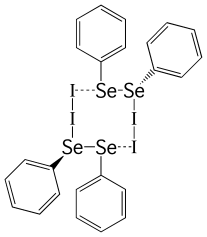

Figure 1. The structure of $Ph_2Se_2I_2$ as described by du Mont et al.[13]

Diphenyl ditelluride reacts rapidly with diiodine to produce an intensely violet-black product. Elemental analysis of this material revealed the stoichiometry "PhTeI", suggesting a product analogous to $Ph_2Se_2I_2$ from du Mont et al.[9] We were nevertheless interested in crystallographically characterizing the compound for comparative purposes. The X-ray crystal

[*] Dr. S. M. Godfrey, P. D. Boyle, W. I. Cross, Prof. Dr. C. A. McAuliffe, Dr. R. G. Pritchard, Dr. S. Sarwar, Dr. J. M. Sheffield
Department of Chemistry
University of Manchester Institute of Science and Technology
Manchester, M60 1QD (UK)
Fax: (+44) 161-228-1250
E-mail: stephen.m.godfrey@umist.ac.uk

  0570-0833/00/3910-1796 $ 17.50+.50/0